

Sliding Mode Control

Gitopoulos Giorgos, 9344

Control III @ ECE AUTH, January 2022

1. Introduction

The current project deals with the *robust control* of a given system with uncertainties, using **sliding mode control**, for both **regulation** and **tracking**. The system will be simulated using *MATLAB* in order to analyze its behavior under the effect of the designed controller and the results will be presented.

2. System

We assume the following robotic arm with two rotational joints:

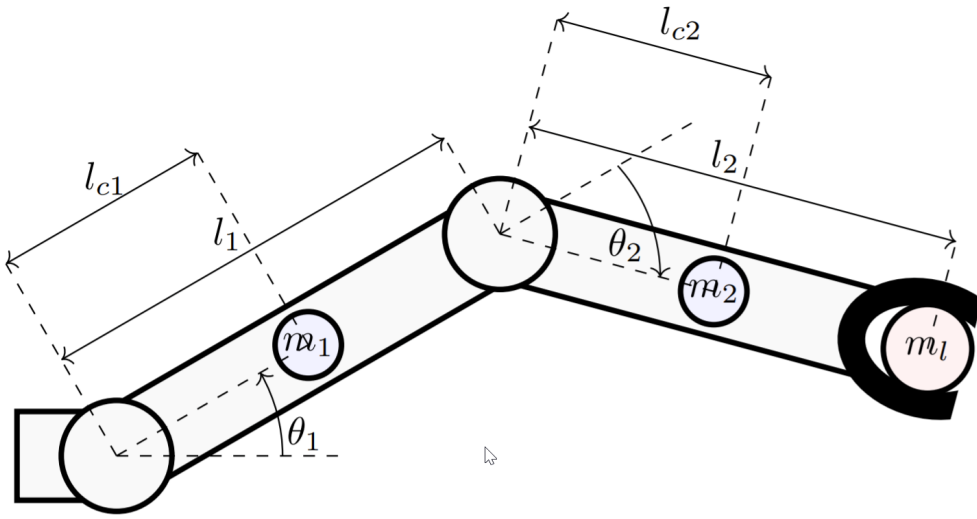


Figure 1: Robotic arm system representation

The angles θ_1 and θ_2 are the rotation angles of the two joints respectively, l_1 and l_2 are the lengths of the two parts of the arm and m_1 and m_2 are the masses of the two parts gathered in the center of mass of each part respectively. The centers of mass are considered to be placed l_{c1} and l_{c2} after each joint. The arm holds a mass m_l , just as in figure 1.

If we assume

$$\begin{cases} q_1 = \theta_1 \\ q_2 = \theta_2 \end{cases}$$

so that

$$q = [\theta_1 \ \theta_2]^T \quad (1)$$

the plant of the system will be

$$H(q)\ddot{q} + C(q, \dot{q})\dot{q} + g(q) = u \quad (2)$$

In the previous equation, H is the 2×2 , positive-definite and symmetric inertia matrix of the robotic arm:

$$H(q) = \begin{bmatrix} h_{11} & h_{12} \\ h_{12} & h_{22} \end{bmatrix}$$

with

$$\begin{aligned} h_{11} &= m_1 l_{c1}^2 + m_2 (l_{c2}^2 + l_1^2 + 2l_1 l_{c2} \cos q_2) + m_l (l_2^2 + l_1^2 + 2l_1 l_2 \cos q_2) + I_1 + I_2 \\ h_{12} &= m_2 l_{c2} (l_{c2} + l_1 \cos q_2) + m_l l_2 (l_2 + l_1 \cos q_2) + I_2 \\ h_{22} &= l_{c2}^2 m_2 + l_2^2 m_l + I_2 \end{aligned}$$

where I_1 and I_2 are the moments of inertia of each part respectively. The matrix C is defined as

$$C(q, \dot{q}) = \begin{bmatrix} -l_1 (m_2 l_{c2} + m_l l_2) \sin q_2 \dot{q}_2 & -l_1 (m_2 l_{c2} + m_l l_2) \sin q_2 (\dot{q}_2 + \dot{q}_1) \\ l_1 (m_2 l_{c2} + m_l l_2) \sin q_2 \dot{q}_1 & 0 \end{bmatrix}$$

and the vector g as

$$g(q) = \begin{bmatrix} (m_2 l_{c2} + m_l l_2) g \cos(q_1 + q_2) + (m_2 l_1 + m_l l_1 + m_1 l_{c1}) g \cos q_1 \\ (m_2 l_{c2} + m_l l_2) g \cos(q_1 + q_2) \end{bmatrix}$$

The values of the known parameters of the system are presented in the following table:

parameter	value
m_1	6 kg
m_2	4 kg
l_1	0.5 m
l_2	0.4 m
g	9.81 m/s ²

Table 1: Values of known parameters

The following parameters are unknown, but we know their lower and upper bounds:

parameter	lower bound	upper bound
l_{c1}	0.1 m	0.4 m
l_{c2}	0.05 m	0.3 m
I_1	0.02 kg m ²	0.5 kg m ²
I_2	0.01 kg m ²	0.15 kg m ²
m_l	0 kg	2 kg

Table 2: Bounds of unknown parameters

3. Controller design

The controller will be designed according to *sliding mode control* method. Firstly we solve (2) for \ddot{q} :

$$H\ddot{q} + C\dot{q} + g = u \Rightarrow$$

$$\ddot{q} = -H^{-1} (C\dot{q} - g + u) \quad (3)$$

Note that H^{-1} exists and it is positive-definite, as H is positive-definite.

We also define the system state error

$$e = e(t) = q(t) - q_d(t) \in \mathbb{R}^{2 \times 1}$$

where $q_d(t) \in \mathbb{R}^{2 \times 1}$ is the desired system state at a time moment t . In the *regulation* process, q_d will be constant, while in *tracking* it will represent the desired signal to be tracked. For our theoretical analysis, we considered the generic case, where q_d is not constant (*tracking*). Note that in terms of convenience, we will represent all the signals of our system without their variable indicator. For example, $q(t)$ is represented as q and $H(q)$ as H .

We also have

$$\dot{e} = \dot{q} - \dot{q}_d \in \mathbb{R}^{2 \times 1}$$

and

$$\ddot{e} = \ddot{q} - \ddot{q}_d \in \mathbb{R}^{2 \times 1}$$

Now, we define the *sliding surface*

$$s = s(\dot{e}, e) = \dot{e} + \Lambda e = [0 \ 0]^T, \quad \Lambda \in \mathbb{R}^{2 \times 2} \Rightarrow$$

$$\dot{e} = -\Lambda e \Rightarrow$$

$$e \rightarrow 0 \quad \text{for } \Lambda > 0$$

So, if we force our system to the surface $s = 0$, we guarantee that the system will tend to the desired behavior. We assume the *Lyapunov* function candidate

$$V(s) = \frac{1}{2} s^T s = \frac{1}{2} [s_1 \ s_2] [s_1 \ s_2]^T = \frac{1}{2} s_1^2 + \frac{1}{2} s_2^2 \Rightarrow$$

$$\dot{V}(s) = s_1 \dot{s}_1 + s_2 \dot{s}_2 = s^T \dot{s} \quad (4)$$

We demand

$$\dot{V}(s) \leq 0 \Leftrightarrow$$

$$s^T \dot{s} \leq 0 \quad (5)$$

with equality only for $s = 0$.

We just have to design a control input u , so that the system satisfies (5).

We have

$$\begin{aligned} \dot{s} &= \ddot{e} + \Lambda \dot{e} = \ddot{q} - \ddot{q}_d + \Lambda \dot{e} \Rightarrow \\ \dot{s} &= -H^{-1}(C\dot{q} + g - u) - \ddot{q}_d + \Lambda \dot{e} \end{aligned} \quad (6)$$

and we define the equivalent input u_{eq} for $\dot{s} = 0$, so from (6) we get

$$u_{eq} = C\dot{q} + g + H\ddot{q}_d - H\Lambda \dot{e}$$

and we use some parameter estimations in the bounds of table 2 for the unknown parameters of u_{eq} , so we have

$$\hat{u}_{eq} = \hat{C}\dot{q} + \hat{g} + \hat{H}\ddot{q}_d - \hat{H}\Lambda \dot{e}$$

In order to reduce chattering, we will use \hat{u}_{eq} in our controller. So, according to *sliding mode control*, the control input will be

$$u = \hat{u}_{eq} - \rho \odot [\text{sat}(s_1, \varepsilon) \text{ sat}(s_2, \varepsilon)]^T \quad (7)$$

where $\rho \in \mathbb{R}^{2 \times 1}$ will be defined later and

$$\text{sat}(x) = \begin{cases} x/\varepsilon, & |x| \leq \varepsilon \\ 1, & x > \varepsilon \\ -1, & x < -\varepsilon \end{cases}$$

Replacing (7) in (2) we get

$$\begin{aligned} H\ddot{q} + C\dot{q} + g &= \hat{C}\dot{q} + \hat{g} + \hat{H}\ddot{q}_d - \hat{H}\Lambda \dot{e} - \rho \odot [\text{sat}(s_1, \varepsilon) \text{ sat}(s_2, \varepsilon)]^T \Rightarrow \\ H\ddot{q} &= \hat{C}\dot{q} + \hat{g} + \hat{H}\ddot{q}_d - \hat{H}\Lambda \dot{e} - \rho \odot [\text{sat}(s_1, \varepsilon) \text{ sat}(s_2, \varepsilon)]^T - C\dot{q} - g \Rightarrow \\ H\ddot{q} - H\ddot{q}_d + H\Lambda \dot{e} &= (\hat{H} - H)\ddot{q}_d + (\hat{C} - C)\dot{q} + (\hat{g} - g) - (\hat{H} - H)\Lambda \dot{e} - \rho \odot [\text{sat}(s_1, \varepsilon) \text{ sat}(s_2, \varepsilon)]^T \Rightarrow \\ H(\ddot{q} - \ddot{q}_d + \Lambda \dot{e}) &= \tilde{H}(\ddot{q}_d - \Lambda \dot{e}) + \tilde{C}\dot{q} + \tilde{g} - \rho \odot [\text{sat}(s_1, \varepsilon) \text{ sat}(s_2, \varepsilon)]^T \Rightarrow \\ H\dot{s} &= \tilde{H}(\ddot{q}_d - \Lambda \dot{e}) + \tilde{C}\dot{q} + \tilde{g} - \rho \odot [\text{sat}(s_1, \varepsilon) \text{ sat}(s_2, \varepsilon)]^T \end{aligned} \quad (8)$$

where

$$\begin{cases} \tilde{H} = \hat{H} - H \\ \tilde{C} = \hat{C} - C \\ \tilde{g} = \hat{g} - g \end{cases}$$

are the error matrices between the estimations of system matrices and the real system matrices. From (9), multiplying the two parts of the equation by left with H^{-1} and subsequently multiplying by left with s^T , we get

$$s^T \dot{s} = s^T H^{-1} [\tilde{H}(\ddot{q}_d - \Lambda \dot{e}) + \tilde{C}\dot{q} + \tilde{g} - \rho \odot [\text{sat}(s_1, \varepsilon) \text{ sat}(s_2, \varepsilon)]^T]$$

We select

$$\rho = \tilde{H}_{max} |\ddot{q}_d - \Lambda \dot{e}| + \tilde{C}_{max} |\dot{q}| + \tilde{g}_{max} + [c \ c]^T \quad (9)$$

where \tilde{H}_{max} , \tilde{C}_{max} and \tilde{g}_{max} are the system matrices with maximum values in all of their elements and $|v| = [|v_1| \ |v_2|]^T$ for a vector $v \in \mathbb{R}^2$. The maximum values of the elements of the matrices occur for the maximum values of the unknown parameter errors:

$$\begin{cases} \tilde{l}_{c1max} = 0.3 \\ \tilde{l}_{c2max} = 0.25 \\ \tilde{I}_{1max} = 0.48 \\ \tilde{I}_{2max} = 0.014 \\ \tilde{l}_{m1max} = 2 \end{cases}$$

according to table 2, as it can be proved that they are increasing with respect to those errors. Replacing (9) in (8) we can reach the inequality

$$s^T \dot{s} \leq -|s^T| |H^{-1}| [c \ c]^T, \quad c > 0 \quad (10)$$

$$\Rightarrow s^T \dot{s} \leq 0$$

with equality only for $s = 0$, so the desired condition (5) is satisfied and $s \rightarrow 0$. Thus, the system slides through $s = 0$ and $q \rightarrow q_d$. The control goal has been achieved.

4. Simulation

The system simulated in *MALTA*B with initial conditions

$$\begin{cases} q_0 = [\frac{\pi}{3} \ \frac{\pi}{3}]^T \\ \dot{q}_0 = [0 \ 0]^T \end{cases}$$

For the real system plant the following values of the unknown parameters were used:

parameter	value
l_{c1}	0.2 m
l_{c2}	0.1 m
I_1	0.43 kg m^2
I_2	0.05 kg m^2
m_i	0.5 kg

Table 3: Real values of unknown parameters

Note that the values of table 3 are considered as unknown, so they were not used in the controller implementation. They were only used to simulate the behavior of the real system. The system was simulated in two different cases: **regulation**, where the control goal was to make the system state vector q to converge to a desired constant state vector q_d , as $t \rightarrow \infty$ and **tracking**, where the control goal was to make the system state vector q to track a reference signal $q_d(t)$, as $t \rightarrow \infty$.

4.1. Regulation

In the first case, we assume

$$\begin{cases} q_d = [\frac{\pi}{2} \ -\frac{\pi}{3}]^T \\ \dot{q}_d = [0 \ 0]^T \\ \ddot{q}_d = [0 \ 0]^T \end{cases}$$

and we set these values in the control input u . The parameter ε of the *saturation* function was set equal to the value 0.05, which provided satisfying results. The further analysis of this parameter is out of scope of this project. Also, we select $c = 0.5$. The effect of this parameter will be discussed later. The selection of matrix Λ of the *sliding surface* was crucial for the system behavior. After tuning, the selected matrix was

$$\Lambda = \begin{bmatrix} 5 & 0 \\ 0 & 5 \end{bmatrix}$$

We will present the system behavior through some diagrams for the selected parameters c and Λ and then we will compare the results with some other values of the parameters.

4.1.1. Results for the selected parameters

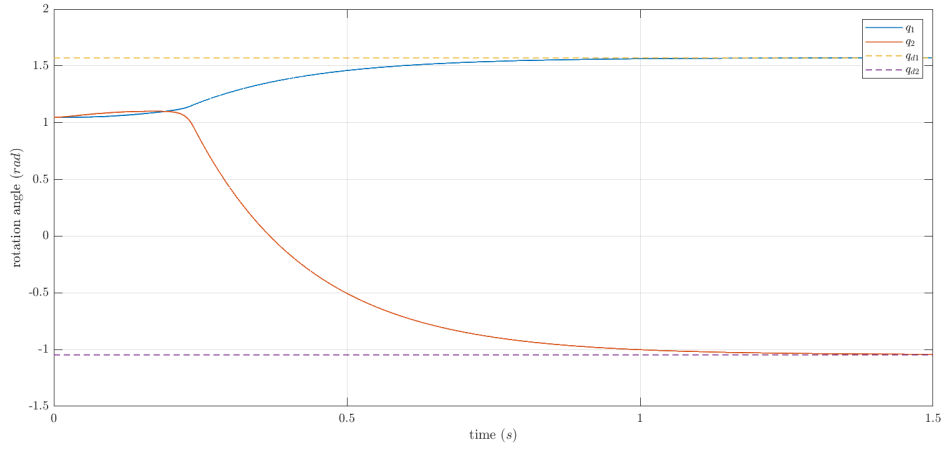


Figure 2: Rotation angles with respect to time

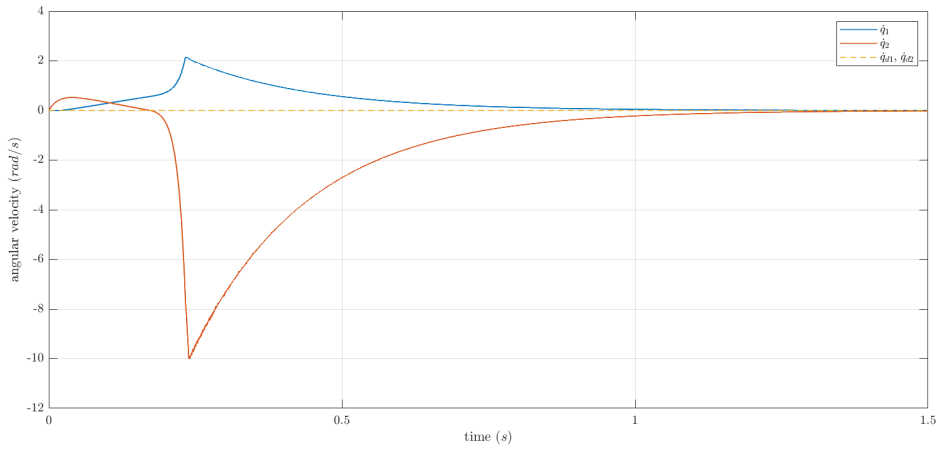


Figure 3: Angular velocities with respect to time

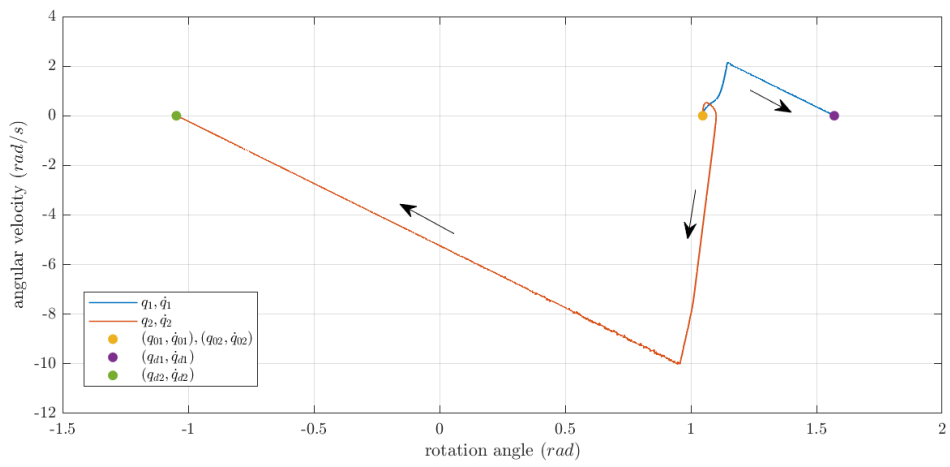


Figure 4: Phase plane of system states

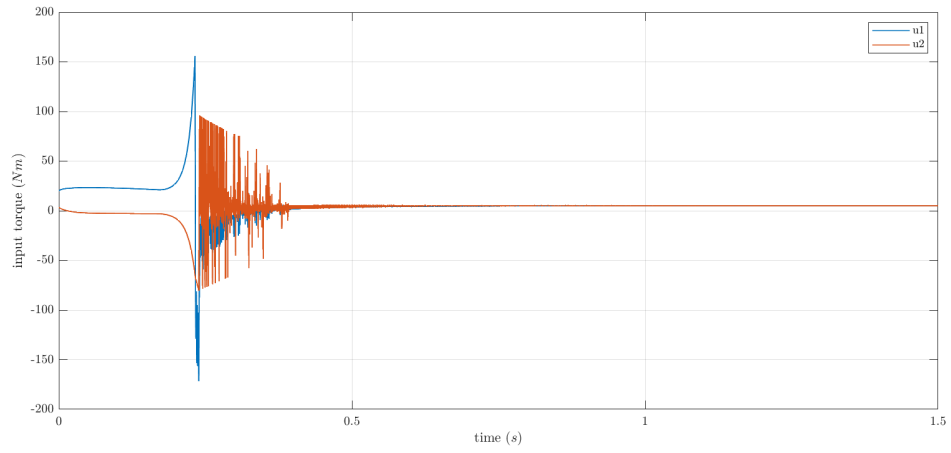


Figure 5: Control input with respect to time

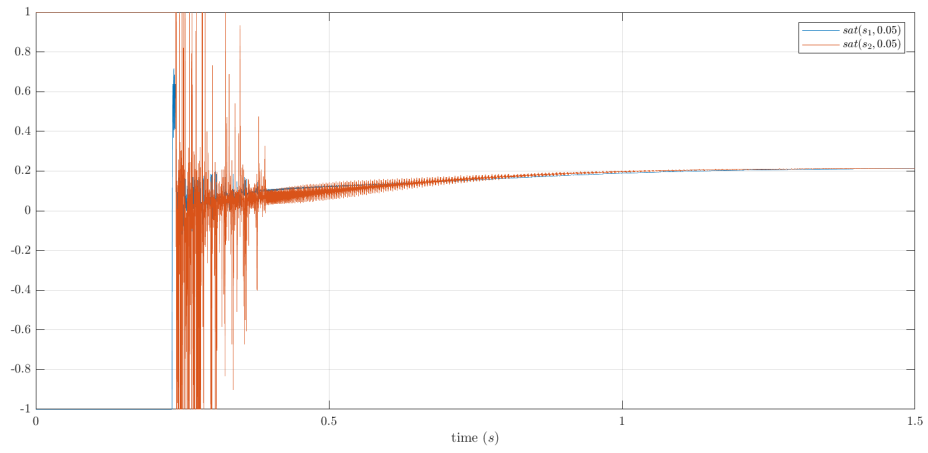


Figure 6: Saturation function of controller with respect to time

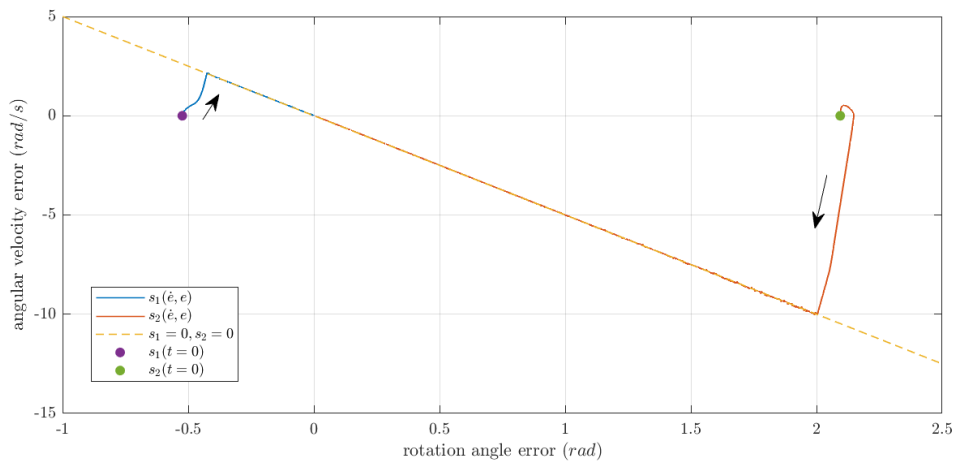


Figure 7: Convergence to sliding surface

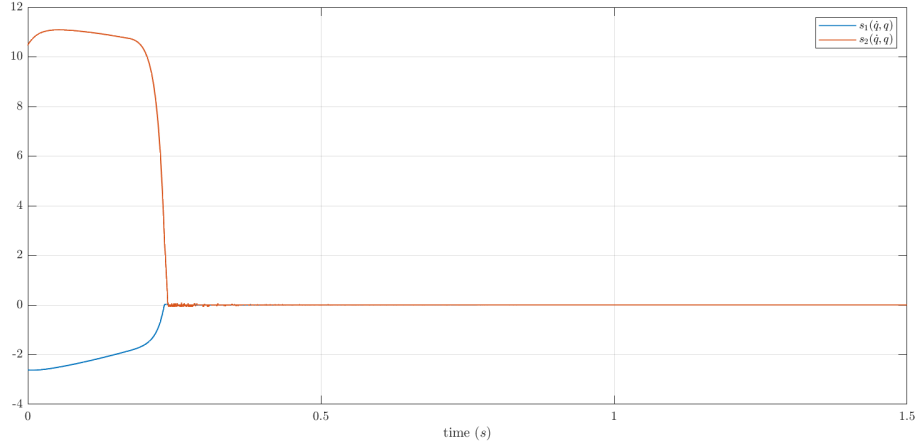


Figure 8: Surface $s(\dot{q}, q)$ with respect to time

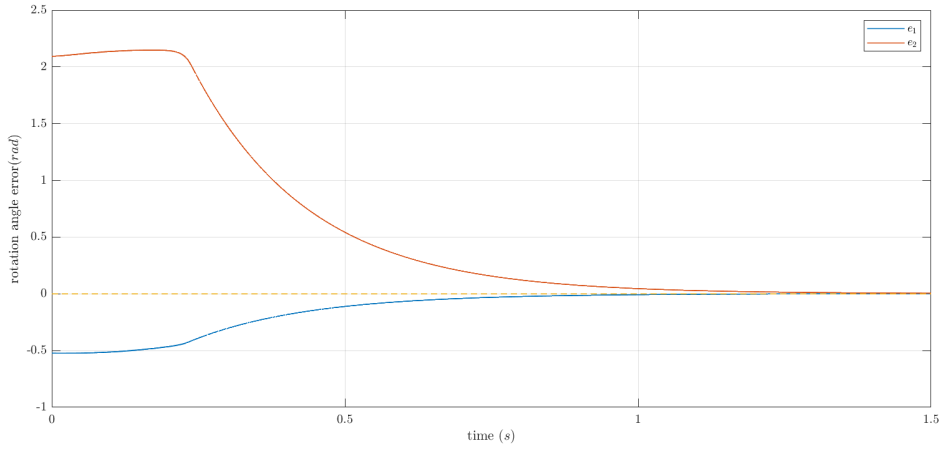


Figure 9: State error with respect to time

- In figure 2, we can see that the system rotation angles converge to the desired values fast enough without undesirable behavior (overshoot, oscillation, etc).
- In figure 3, we notice that the angular velocities converge to the desired values too.
- In figure 5, we can see the discontinuities in the control input due to saturation function (figure 6). These discontinuities disappear when s gets into the $|\varepsilon|$ bounds and the control input becomes more stable, tending to a constant value while $t \rightarrow \infty$.
- All the signals of the system are bounded (figures 1,2, 5).
- The theoretical *rise times* for s_1 and s_2 are

$$\begin{cases} t_{r1} \leq \frac{|s_1(0)|}{c} = \frac{2.618}{0.5} = 5.236s \\ t_{r2} \leq \frac{|s_2(0)|}{c} = \frac{10.472}{0.5} = 20.944s \end{cases}$$

which is clearly validated by figure 8, as we see that $s(\dot{q}, q)$ reaches $s = 0$ much faster.

- In figure 5 we can see the *phase plane* of the system states as they converge to the equilibrium point.
- In figure 7 the convergence of the system to the *sliding surface* is visible. In figure 8 we can see the time when the system reaches the *sliding surface*. Since that time (about 0.25 seconds), the state errors start converge to zero, validating our theoretical expectations, as the error slides through the surface $s = 0$.
- Moreover, by the time the system reaches the *sliding surface*, the power of the input torque (figure 5) starts becoming stable.

4.1.2. Parameter c analysis

From (10) we can export that the increase of parameter c can make the *Lyapunov* derivative more negative, so the system will reach faster $s = 0$ state. We provide an example for $c = 10$ (larger than the selected $c = 0.5$) and Λ equal to the selected:

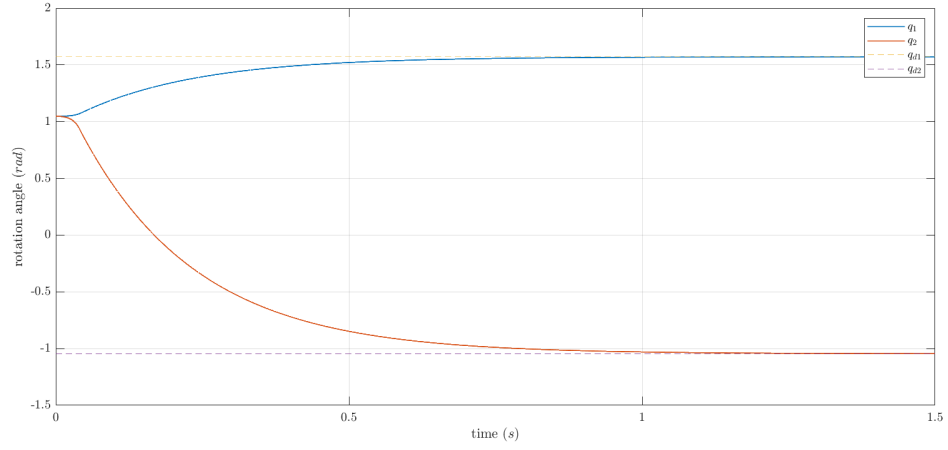


Figure 10: Rotation angles with respect to time for $c = 10$

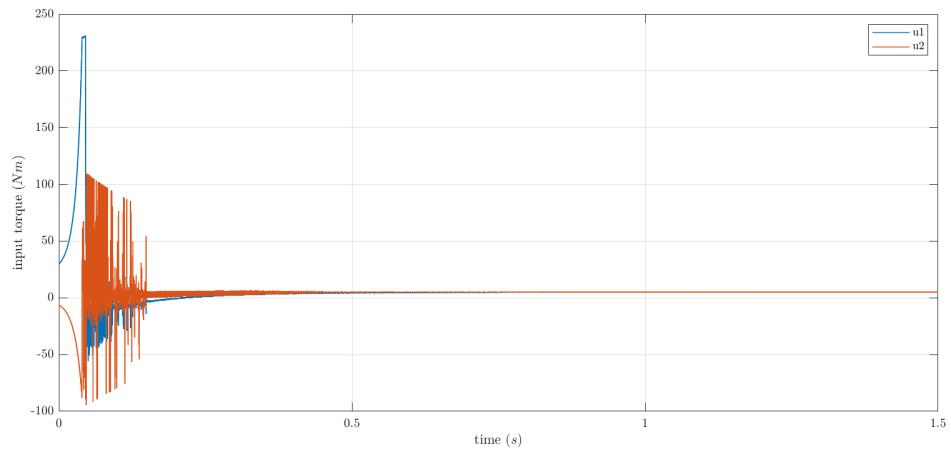


Figure 11: Control input with respect to time for $c = 10$

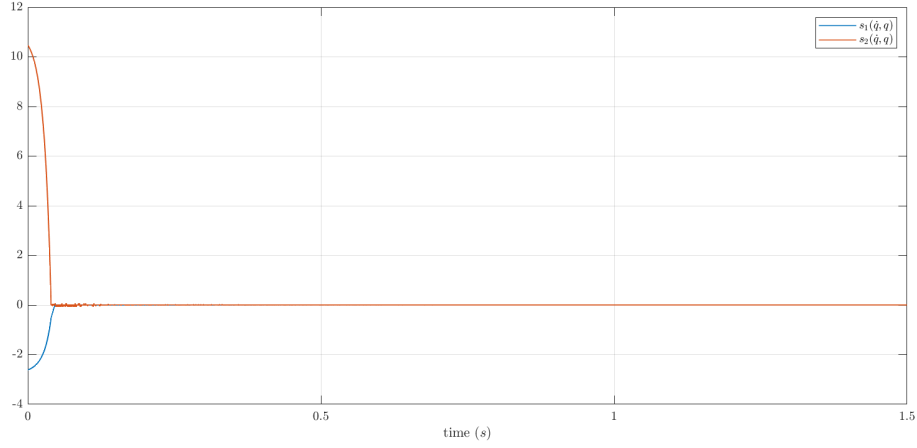


Figure 12: Surface $s(\dot{q}, q)$ with respect to time for $c = 10$

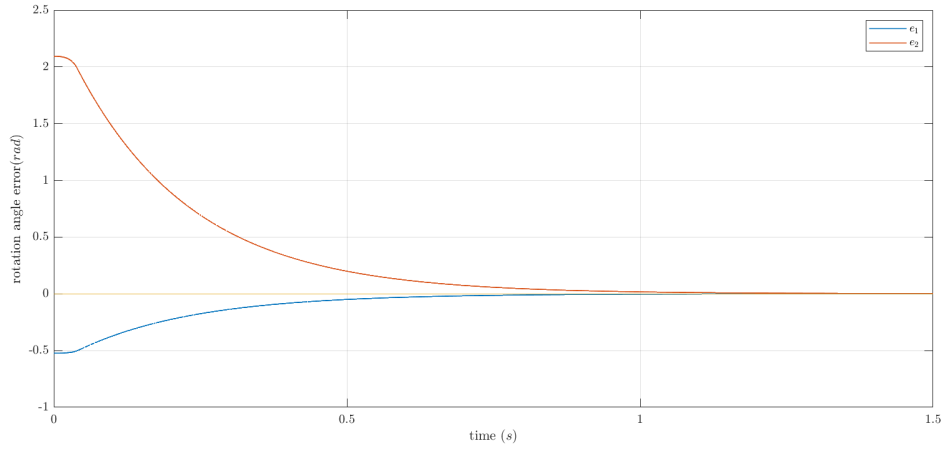


Figure 13: State error with respect to time for $c = 10$

Comparing figures 8 and 12, our theoretical approach is validated, as $s(\dot{q}, q)$ converges much faster to zero for the increased value of c . However, comparing figures 2 and 10 we see that the improvement in system state converge time is not important, as parameter c affect the system speed until it reaches $s = 0$ surface. Since then, the converge speed is defined by some parameters that will be analyzed in the next subsection. Overall, increase of parameter c only achieves to reduce the time until the state error starts decreasing (figure 13) and increases the maximum strength of control signal (figure 11). As a result, it was preferred to keep the parameter at the value $c = 0.5$.

4.1.3. Parameter matrix Λ analysis

Now, we will examine some other candidate matrices Λ with constant $c = 0.5$. We assume

$$\Lambda = \begin{bmatrix} \lambda_1 & 0 \\ 0 & \lambda_2 \end{bmatrix}$$

In the previous results, we selected $\lambda_1 = \lambda_2 = 5$. From the definition of the *sliding surface* we get

$$\dot{e} = -\Lambda e \Rightarrow$$

$$\begin{cases} \dot{e}_1 = -\lambda_1 e_1 \\ \dot{e}_2 = -\lambda_2 e_2 \end{cases}$$

so it is obvious that λ_1 and λ_2 determine the speed of the error convergence to zero, once the system reaches the *sliding surface*. For $\lambda_1 = \lambda_2 = 0.5$ we present the following diagram:

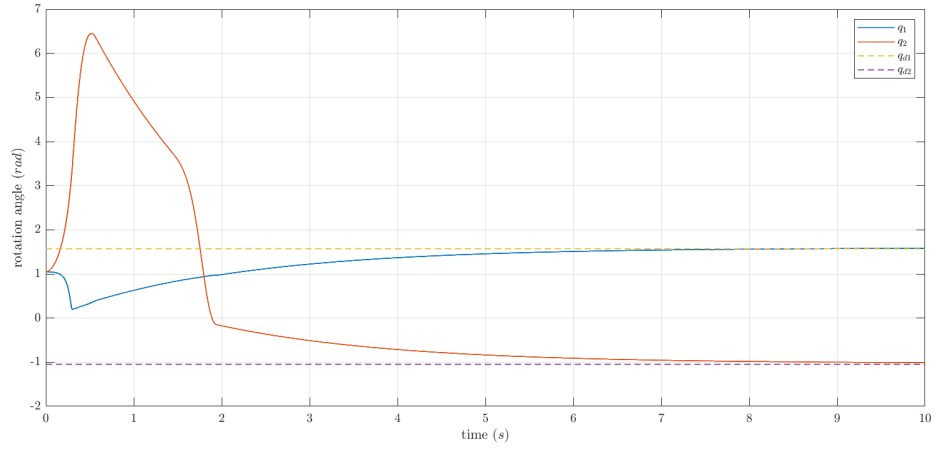


Figure 14: *Rotation angles with respect to time for $\lambda_1 = \lambda_2 = 0.5$*

We can notice that the converge is much slower in comparison with figure 2 ($\lambda_1 = \lambda_2 = 5$), as expected. Also, q_2 presents high overshoot. We conclude that these values of parameters lead to undesirable behavior of the system.

Now we set $\lambda_1 = \lambda_2 = 25$ and we expect faster convergence:

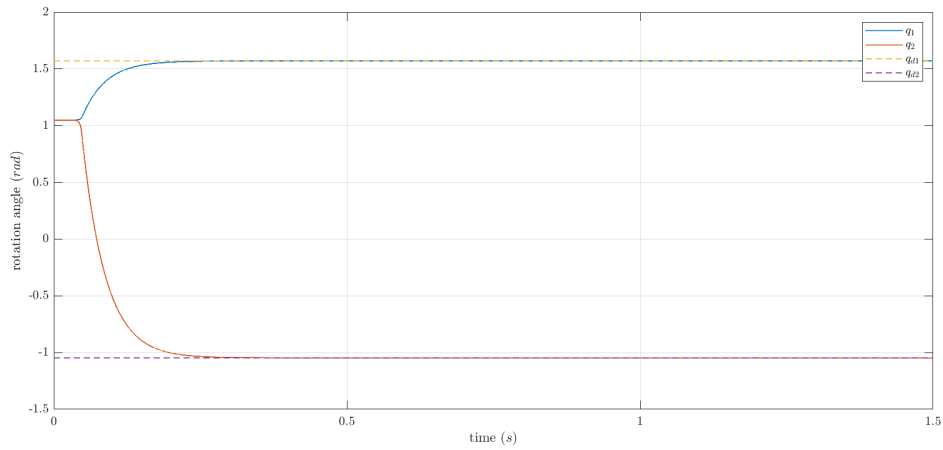


Figure 15: *Rotation angles with respect to time for $\lambda_1 = \lambda_2 = 25$*

Actually our prediction is confirmed and the converge is even faster than figure 2. However, if we look at the control input:

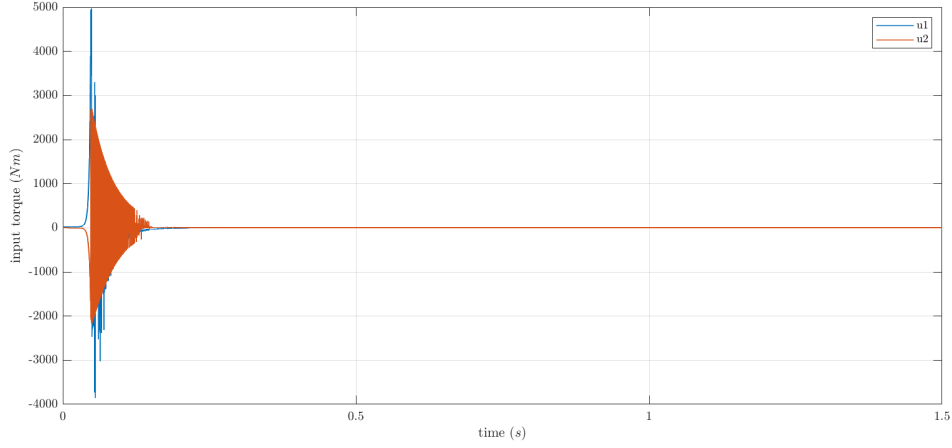


Figure 16: Control input with respect to time for $\lambda_1 = \lambda_2 = 25$

we can see that it takes much larger values compared to figure 5, until the system reaches the *sliding surface*. This is often unwanted, as the controller demands huge amount of power leading to problems like high energy consumption, construction cost, etc. Taken into account criteria like these, we tuned the system with respect to parameters λ_1 and λ_2 and selected $\lambda_1 = \lambda_2 = 5$.

4.2. Tracking

Now we assume the desired state orbit

$$q_d = \begin{bmatrix} \frac{\pi}{4} + \frac{\pi}{6} \sin(0.2\pi t) \\ -\frac{\pi}{3} + \frac{\pi}{3} \cos(0.2\pi t) \end{bmatrix}$$

The control goal is to make the state vector q to track the orbit q_d as $t \rightarrow \infty$, using *sliding mode control*. As previously, we set in (7) the new desired state vector q_d and we have to select the parameters c and Λ of the control input. After tuning, we selected $c = 10$, $\lambda_1 = 2$ and $\lambda_2 = 5$. The system behavior for these values of parameters is presented below.

4.2.1. Results for the selected parameters

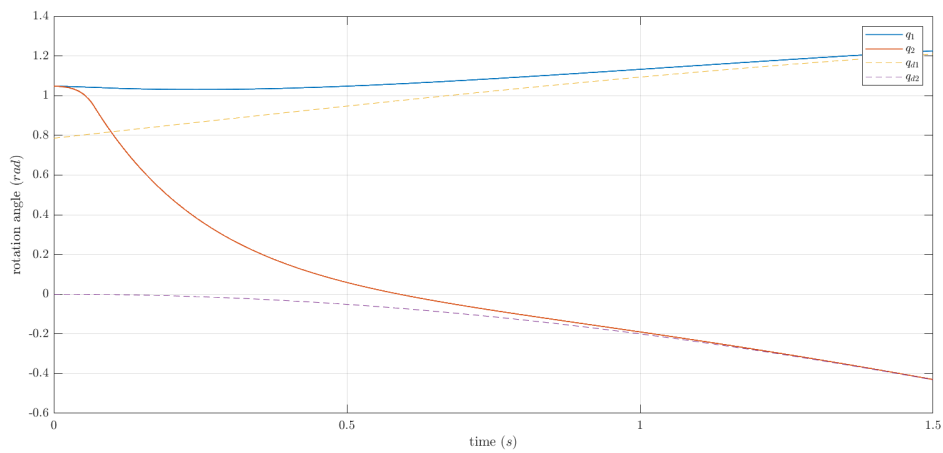


Figure 17: Rotation angles with respect to time

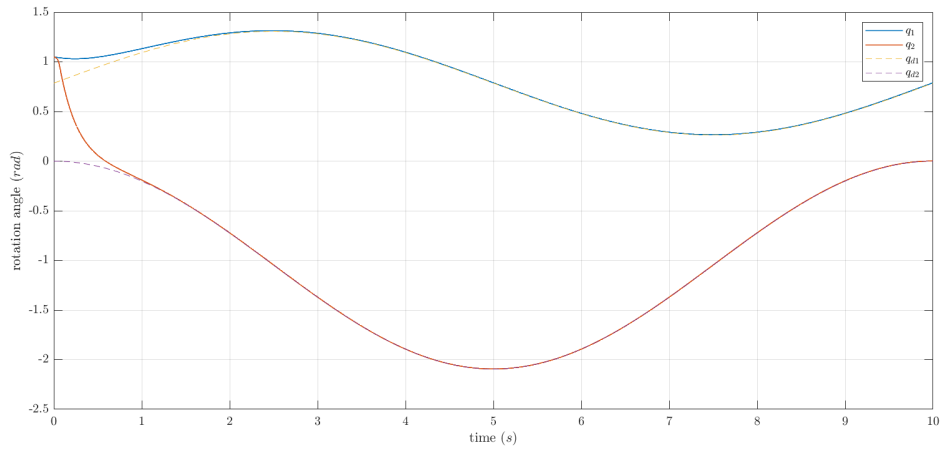


Figure 18: Rotation angles with respect to time - long scale

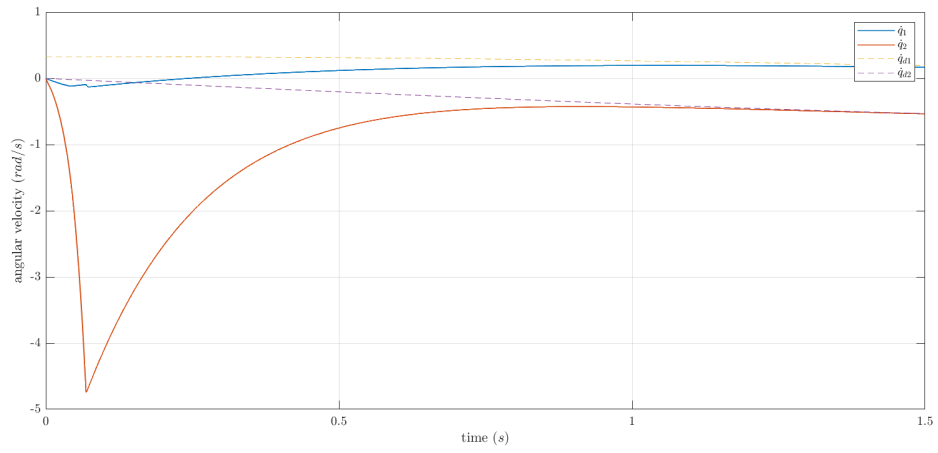


Figure 19: Angular velocities with respect to time

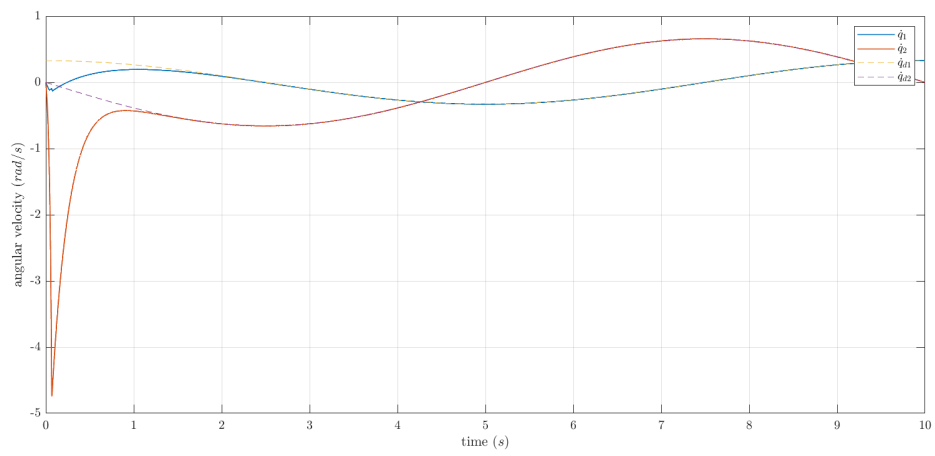


Figure 20: Angular velocities with respect to time - long scale

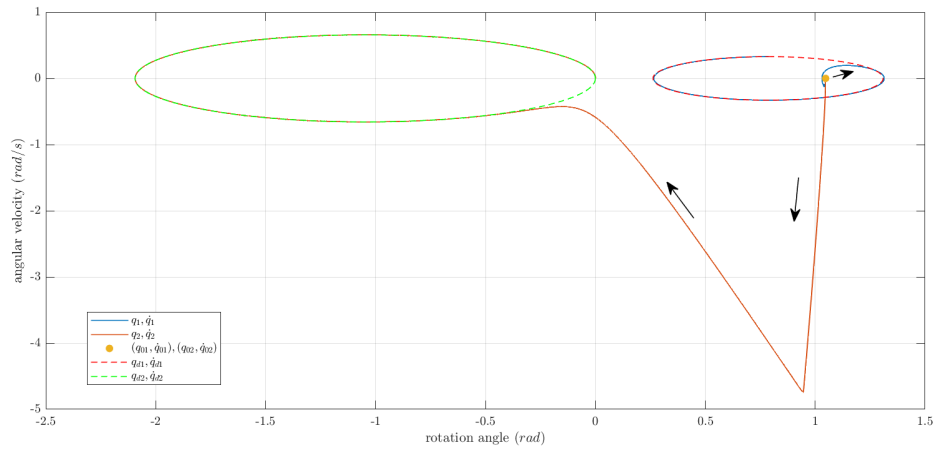


Figure 21: *Phase plane of system states - long scale*

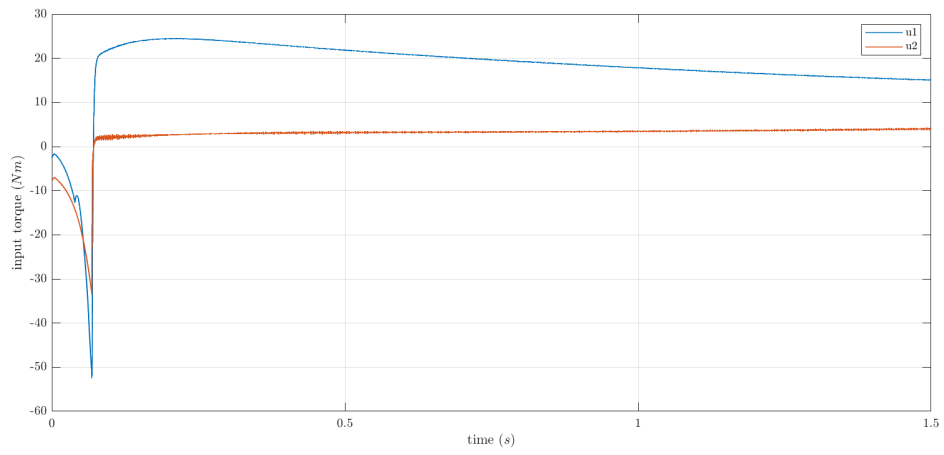


Figure 22: *Control input with respect to time*

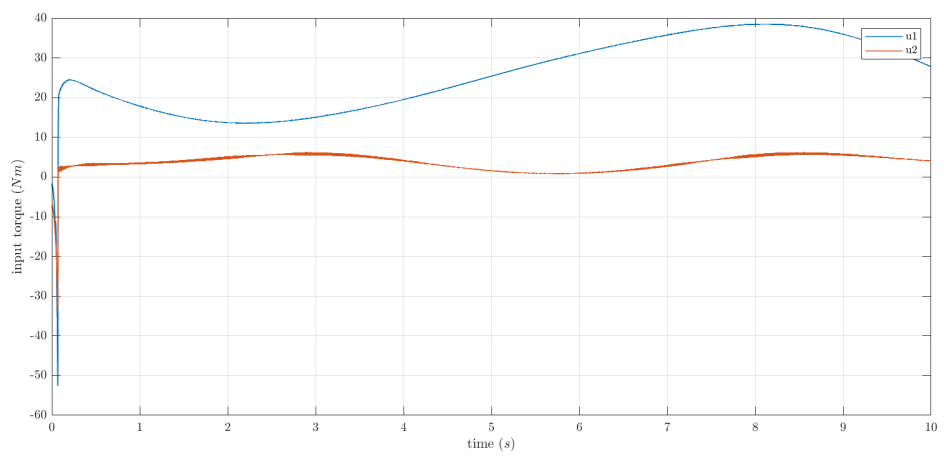


Figure 23: *Control input with respect to time - long scale*

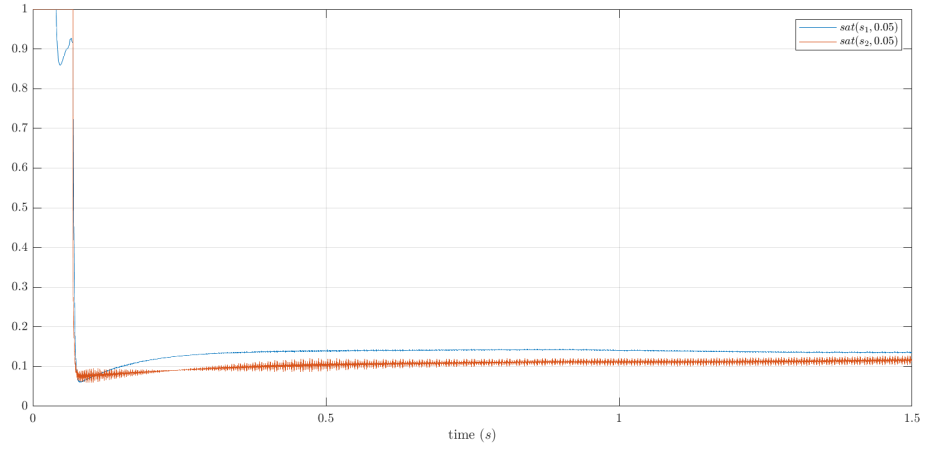


Figure 24: Saturation function of controller with respect to time

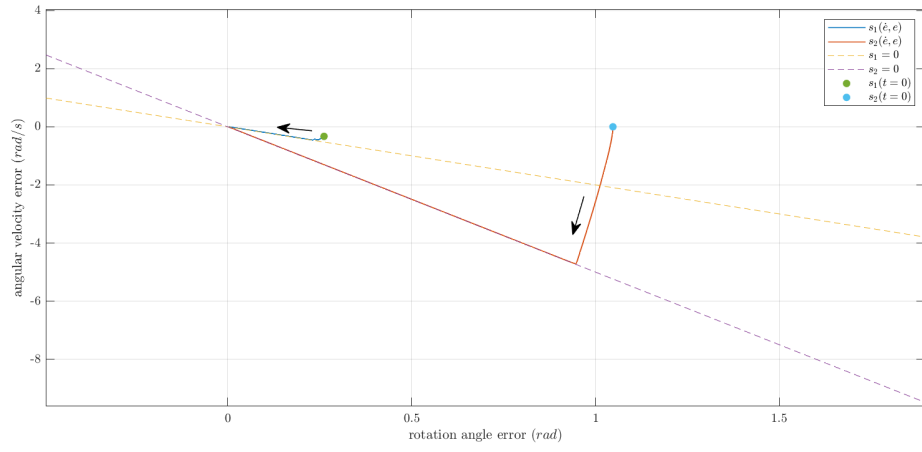


Figure 25: Convergence to sliding surface - long scale

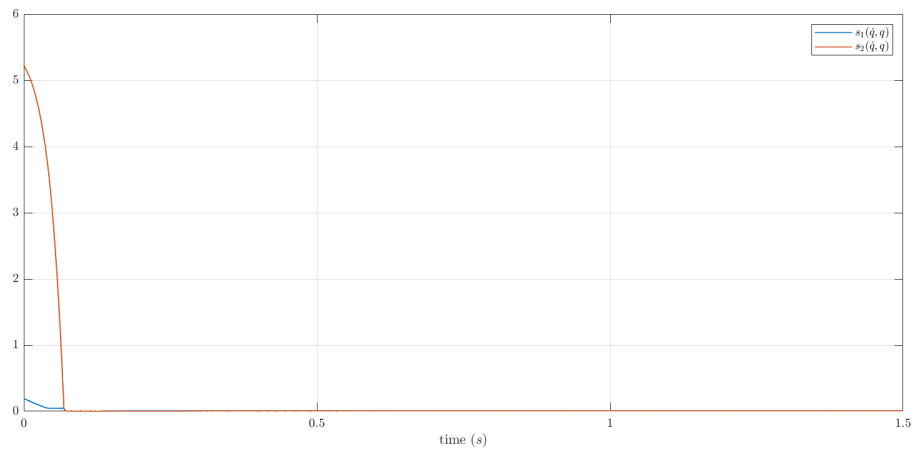


Figure 26: Surface $s(\dot{q}, q)$ with respect to time

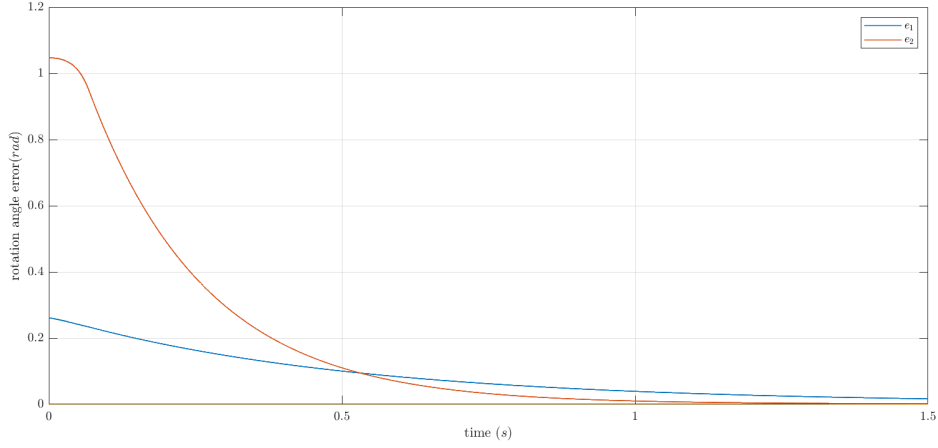


Figure 27: *State error with respect to time*

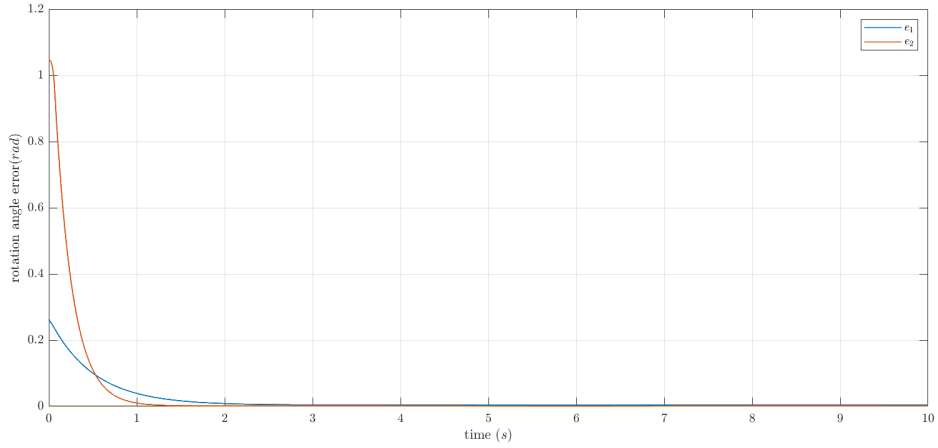


Figure 28: *State error with respect to time - long scale*

- From figures 17, 18, 19 and 20 we can export that the system states track very satisfactorily the desired state orbits and they converge to these orbits in less than 1 second.
- In figure 21, we can observe the phase plane of the system states as they converge to the desired orbits. Since they reach these orbits, they keep moving in them.
- Figures 22 and 23 prove that the control input is satisfactorily bounded and the maximum power is not too high.
- We can conclude that all the signals in the closed loop are bounded.
- In figure 24, we can see that the saturation function becomes much more stable, by the time that the system reaches the $|\varepsilon|$ bounds (figure 26). However, there is still chattering in the saturation function, which leads the control input and thus, the system states to slight chattering too.
- The converge of the system to the $s = 0$ surface can be noticed in figure 25. In contrast with the *regulation* problem, this time we choose different values for λ_1 and λ_2 , which results in two different lines for $s_1 = 0$ and $s_2 = 0$. As we can see in figure 25, each component of $s(\dot{e}, e)$ converges to a different *sliding line*.
- In figure 26, we can see the convergence of the system to $s = 0$ with respect to time. When $s(\dot{e}, e)$ reaches close to zero, the state error starts decreasing (figure 27), as the error slides through the *sliding surface*.

4.2.2. Parameter c analysis

As we explained before, the parameter c defines the speed of convergence to the *sliding surface*. We present the results for $c = 1$ and $c = 25$ separately, with constant $\lambda_1 = 2$ and $\lambda_2 = 5$:

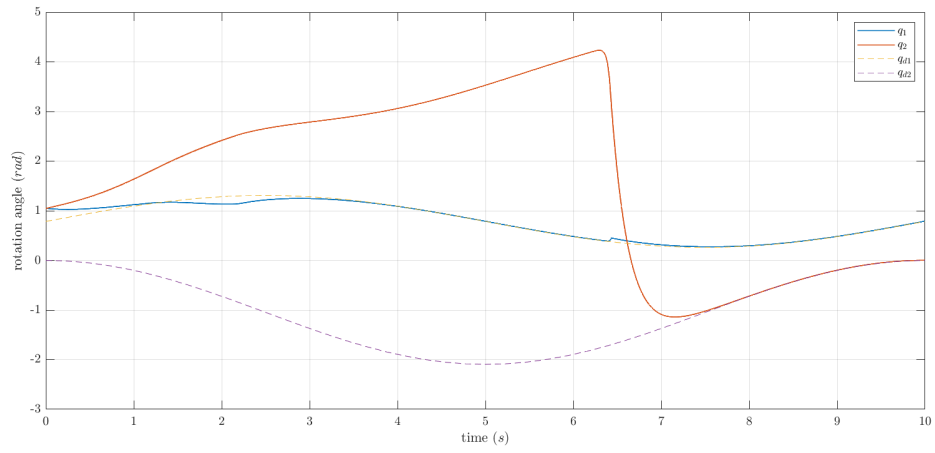


Figure 29: Rotation angles with respect to time for $c = 1$

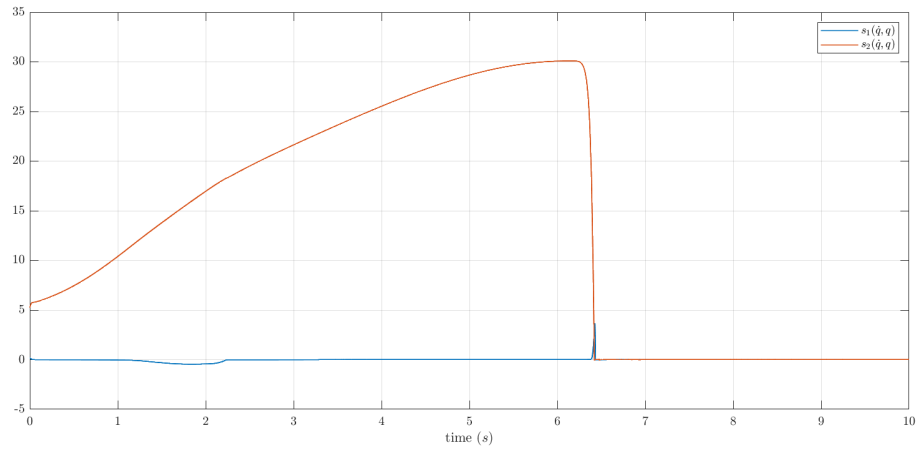


Figure 30: Surface $s(\dot{q}, q)$ with respect to time for $c = 1$

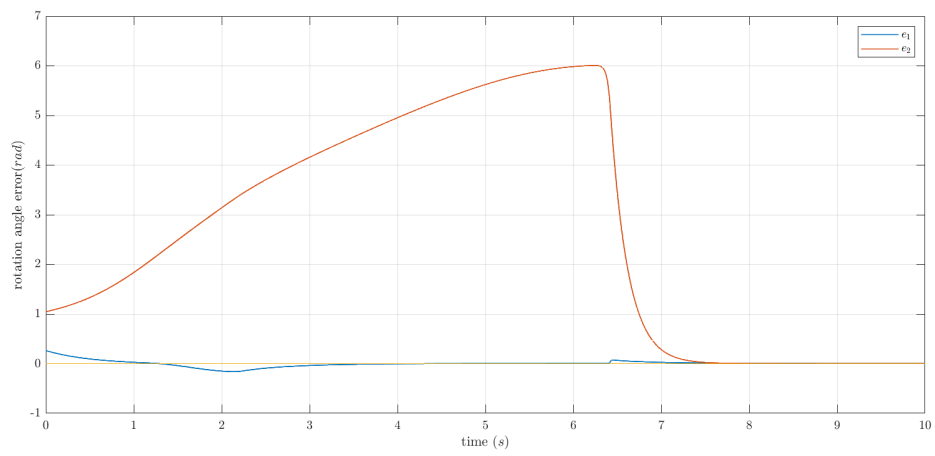


Figure 31: State error with respect to time for $c = 1$

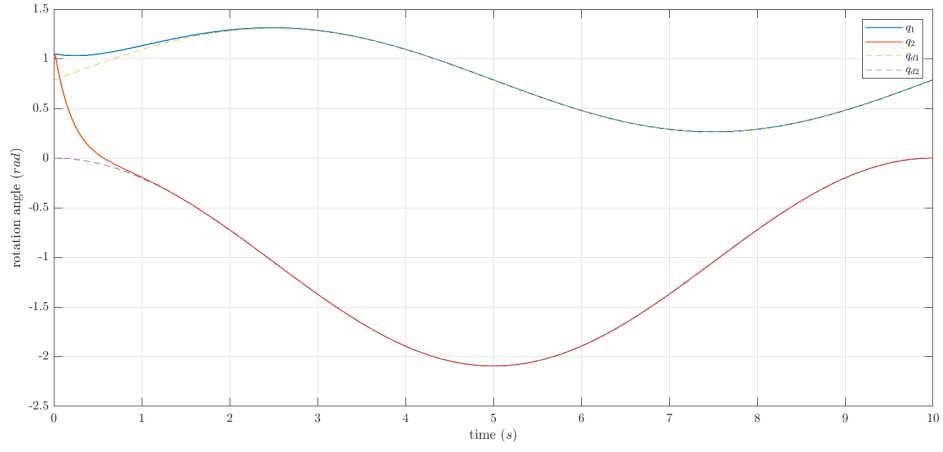


Figure 32: Rotation angles with respect to time for $c = 25$

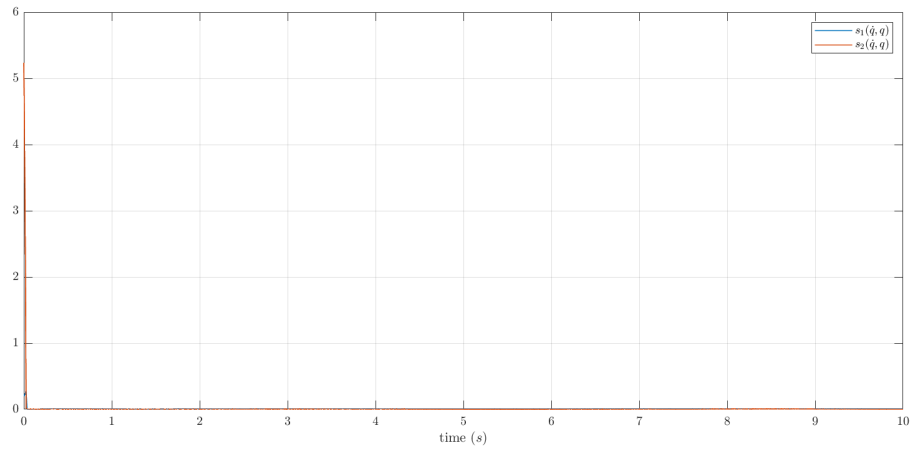


Figure 33: Surface $s(\dot{q}, q)$ with respect to time for $c = 25$

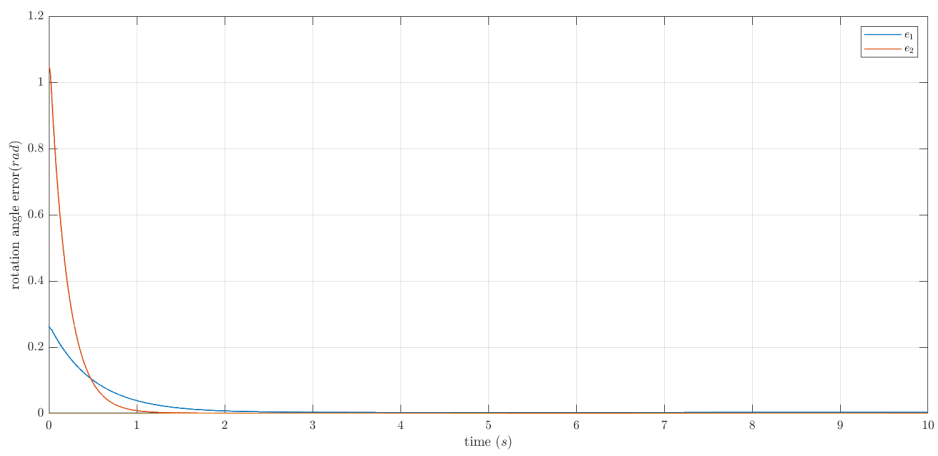


Figure 34: State error with respect to time for $c = 25$

Through figures 29, 30 and 31, we validate our theoretical estimations, as the convergence to the *sliding surface* is delayed for a lower value of c ($c = 1 < 10$). So, the error starts decreasing later in comparison with the case with the selected parameter c ($c = 10$). For $c = 25$, we can notice that the convergence has reached to saturation and cannot be improved further as c increases (figures 32, 34), although $s = 0$ is reached earlier (figure 33).

4.2.3. *Parameter matrix Λ analysis*

According to matrix Λ , we will firstly decrease the values of the matrix and set $\lambda_1 = 0.2$ and $\lambda_2 = 0.5$ with constant $c = 10$. Subsequently, we will increase the values to $\lambda_1 = 10$ and $\lambda_2 = 20$. We present the results below: **TODO**